PROCEEDINGS OF SPIE

SPIEDigitalLibrary.org/conference-proceedings-of-spie

Laser Doppler vibrometry sensors implemented in a silicon photonic integrated circuit for measuring cardiovascular signals on bare skin

Yanlu Li, Soren Aasmul, Andrei Bakoz, Chirag Murendranath Patil, Padraic Morrissey, et al.

Yanlu Li, Soren Aasmul, Andrei Bakoz, Chirag Murendranath Patil, Padraic E. Morrissey, Tracy Wotherspoon, Owen Pullin, Felix Campano Casado, Petr Záruba, Roel Baets, "Laser Doppler vibrometry sensors implemented in a silicon photonic integrated circuit for measuring cardiovascular signals on bare skin," Proc. SPIE 12355, Diagnostic and Therapeutic Applications of Light in Cardiology 2023, 1235507 (14 March 2023); doi: 10.1117/12.2648832

SPIE.

Event: SPIE BiOS, 2023, San Francisco, California, United States

Laser Doppler vibrometry sensors implemented in a silicon photonic integrated circuit for measuring cardiovascular signals on bare skin

Yanlu Li*[a,b], Soren Aasmul[c], Andrei Bakoz[d], Chirag Murendranath Patil[d], Padraic E. Morrissey[d], Tracy Wotherspoon[e], Owen Pullin[e], Felix Campano Casado[e], Petr Záruba[f], Roel Baets[a,b]

[a]Photonics Research Group, Ghent University-imec, Technologiepark-Zwijnaarde 126, 9052, Ghent, Belgium;[b]Center for Nano- and Biophotonics, Ghent University, Technologiepark-Zwijnaarde 126,9052, Ghent, Belgium;[c]Medtronic Bakken Research Center, Endepolsdomein 5, 6229 GW, Maastricht, The Netherlands;[d]Photonic Packaging Group, Tyndall National Institute, Lee Maltings Complex Dyke Parade, T12R5CP, Cork, Ireland;[e]Microchip Technology Inc., Caldicot Limited, Phase 2, Castlegate Business Park, Monmouthshire, NP26 5YW, UK;[f]Argotech a.s., Náchodská 529, 54101 Trutnov, Czech Republic

ABSTRACT

Laser Doppler vibrometer (LDV) sensors can measure skin vibrations originating from propagating superficial arterial pulse waves, which can be used to assess arterial stiffness and identify stenosis and heart failure. A key challenge is to get sufficient diffusely reflected power from bare skin in order to avoid the use of a retroreflective patch. Here we report a prototype, enabled by silicon photonics, that can directly measure the vibrations of bare human skin. We demonstrate a resolution better than 10 pm/sqrt(Hz) when the skin surface is placed at the focal plane of the sensing beams. This result holds great promise for the targeted cardiovascular applications.

Keywords: cardiovascular disease monitoring, Laser Doppler vibrometry, Multi-beam Mach-Zehnder interferometer, photonic integrated circuit, silicon photonics

1. INTRODUCTION

Cardiovascular disease (CVD) is one of the main causes of death in the world nowadays with around 17.8 million deaths reported in 2019 [1]. Many efforts have been made to develop low-cost and easy-to-use methods/devices to monitor CVD systems at early stages so that more people can have better CVD management or prevention [2,3]. We have developed a compact non-invasive optical sensor for CVD monitoring and diagnosis [4]. The core of this sensor is a multi-beam Laser Doppler Vibrometer (LDV) fabricated on a compact silicon photonic integrated circuit [5]. The multi-channel measurement solution measures arterial-pulse-wave-induced skin movements and reduces the alignment effort. The measured data can be used to derive important CVD markers such as pulse wave velocity (PWV), a value that is used to assess arterial stiffness.

Since the skin is a very diffusive scattering surface, retro-reflective (RR) patches have been used to enhance the reflection in our previous work [6]. A custom-made RR patch with micro-glass beads was applied to the skin before each measurement. Based on the experience in our clinical feasibility study, the users suggested avoiding the use of such RR patches due to the additional procedure step and potential measurement errors due to the mass and stiffness of the RR patches. However, without RR patches, the optical reflection back to the LDV was very low. We measured a 30 dB to 40 dB extra loss after removing the RR patches in the skin [6]. Such a strong loss results in a low signal-to-noise ratio (SNR), which renders a measurement on bare skin impossible for most people with these previous demonstrators.

*Email: Yanlu.Li@UGent.be

Diagnostic and Therapeutic Applications of Light in Cardiology 2023, edited by Laura Marcu, Gijs van Soest, Proc. of SPIE Vol. 12355, 1235507
 · 1605-7422 · doi: 10.1117/12.2648832

To reach the goal of eliminating the need for an RR patch, several methods have been implemented in our new prototypes, including changing the wavelength from 1550 nm to 1310 nm, increasing laser optical power and numerical aperture (N.A.) of the LDV, reducing the number of sensing beams and using optimized transimpedance amplifiers. We have analyzed the reasons to use these methods in one of our earlier publications [6]. These improvements are summarized in Table 1. It can be seen that the most powerful methods are the increase of the N.A. of the optical system and the reduction of electronic noise. With these methods, we can increase the SNR to a level sufficient for direct measurements on bare skin.

Table 1. The improvements of the LDV system to reach the goal of direct measurement on bare skins.

Method	**Reasons for the improvement**	**Expected SNR improvement**
Less number of beams: from 6 beams to 4 beams	More power in each beam. Six beams were not necessary, four are enough.	1.5×
Change the sensing wavelength from 1550 nm to 1310 nm	Less optical absorption in the skin due to less absorption by water.	up to 6×
Stronger optical power from the laser sources	Higher sensing power so better SNR	2× to 4×
Better electronics and put TIA closer to the LDV chip	Less noise from electronics	>10×
Change the optical systems and use larger numerical aperture to collect reflections	More reflection power and hence stronger signal strengths.	>36×

2. SYSTEM DESIGN AND MEASUREMENT SETUP

In this section, we will describe the details of the new LDV sensor. First, we will explain the working principle of an on-chip LDV. An LDV is an optical interferometer. One of its optical beams is sent to the device under test (DUT). The reflected light is coupled back into the interferometer and combined with a reference signal. The Doppler frequency shift of the reflected light, which is proportional to the instantaneous velocity of the DUT, can be retrieved from the combined signals with proper demodulation algorithms. Generally, heterodyne methods and homodyne methods [7] can be used. In the on-chip LDV, we are using a homodyne method because of the lack of an efficient frequency shifter on the chip. In homodyne detection, the reflection signal is combined with the reference signal that is routed internally in the LDV chip and has a fixed optical path. The reflection and the reference signals are combined in a 90° hybrid that produces four combined 90° phase shifted signals that are detected in four identical PDs. The photocurrents of the four PDs can be expressed as $PD_k(t) = dc_k + r \cdot \cos(2\pi\phi(t) + k\pi/2), k = 1,2,3,4$. Here we directly retrieve the difference of two signals with 180° phase differences and form two signals:

$$I(t) = PD_4(t) - PD_2(t) = dc_I + 2r \cdot \cos\big(2\pi\phi(t)\big),$$

and

$$Q(t) = PD_3(t) - PD_1(t) = dc_Q + 2r \cdot \sin\,(2\pi\phi(t)).$$

Ideally, the Lissajous curve of the I and Q signals forms a circle centered at (dc_I, dc_Q). The radius of the IQ curve ($Radius = 2r$) is proportional to the strength of the reflected beam, while the phase of each data point in the IQ curve corresponds to the Doppler phase change (integration of Doppler frequency shift) of the reflected signal at that time. With the derived phase/frequency information from the data, we can retrieve the displacement/velocity information of the DUT in the time domain.

In this design, a four-beam on-chip LDV design is used to realize the direct skin measurements. The four optical antennas of the LDV are placed on a line in the LDV chip with a pitch of 0.5 mm. The pitch of the four beams on the target is set to 5 mm. For a confocal lens system, an optical magnification of -10 is needed. However, in combination with the N.A. of the optical antennas on the LDV chip, this magnification results in an N.A. of around 0.009 for the focusing beams to the DUT, which is too small and thus limits the amount of light coupled back into the LDV chip. To solve this problem, four small focusing lenses are placed at the target side to focus the sensing beams again (see Figure 1). This reduces the total spot-size magnification of each beam in this optical system to 2.7, which increases the N.A. to around 0.033 resulting in more light can be collected back into the system. A theoretical prediction of the depth of focus is around ± 0.4 mm.

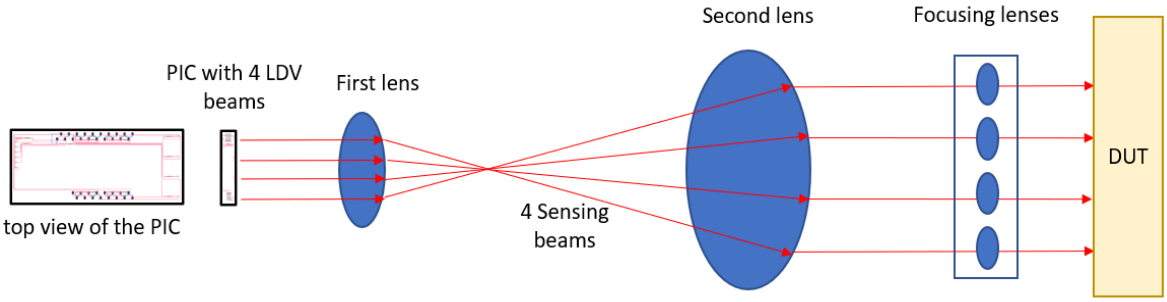

Figure 1. The optical system of the four-beam LDV system.

An image of a packaged sensor head is shown in Figure 2. A micro-optical bench (MOB) with a laser source, an optical isolator, and micro ball lenses is aligned and glued on the LDV chip. Light is coupled from the MOB to the LDV chip vertically via an on-chip grating coupler. The four sensing beams are sent out of the LDV chip via four optical antennas (also based on grating couplers) on the top edge of the LDV chip. The output light beams pass through the glass cover of the package with anti-reflective coatings, then enter the aforementioned optical system and finally reach the DUT. The reflected signals from the DUT are coupled back to the LDV chip via the same optical antennas. The reflected signals are combined with on-chip reference signals and form four I/Q pairs of photocurrent signals for the four channels. These photocurrent signals are then sent to the eight transimpedance amplifiers in the PCB via wire bondings. Short distances between the PDs and the preamplifiers in combination with high gain/low input referred noise transimpedance amplifiers result in a considerably higher SNR than for our previous demonstrator. The preamplified signals are then sent out to external electronics via the pins of the package.

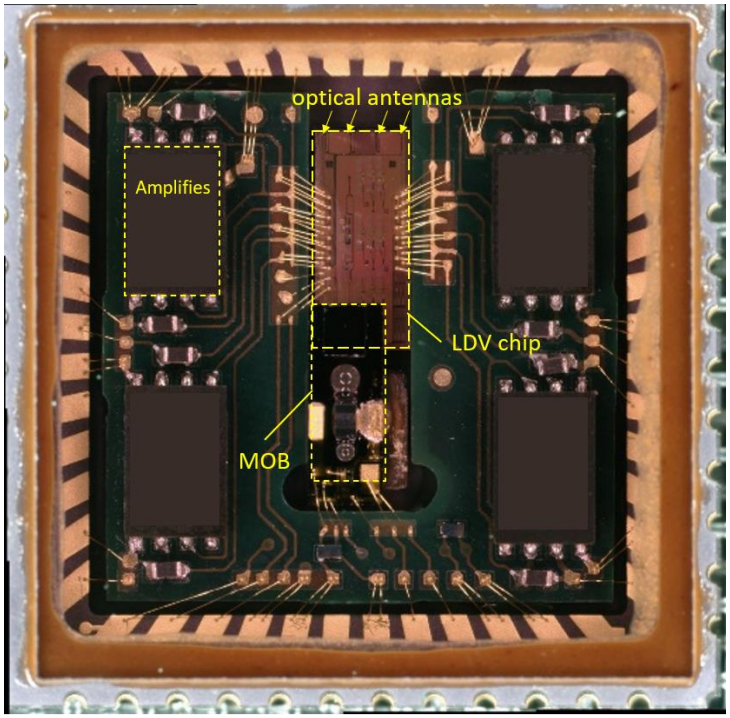

Figure 2. Microscope Image of the packaged LDV chip with preamplifiers. The labels of the amplifiers are removed in this image.

During the test, the packaged sensor head is mounted on a test PCB and aligned with the confocal optical system. The entire system is supported in a cage system to ensure all components are well aligned (see Figure 3:top). A data acquisition (DAQ) system is connected to the photonic package via the test PCB to sample the I and Q signals from the four-channel LDVs. I and Q time series data are stored on the computer during the measurement for later demodulation. The demodulation of the I and Q signals is conducted using a Matlab code, which retrieves the phases of the data points on the IQ curve.

3. MEASUREMENT PROCEDURES, RESULTS, AND DISCUSSIONS

The optical power sent out in each channel is measured with the help of an aspheric lens and an optical power meter (see Figure 3:top). A photo of the setup is shown in Figure 3:bottom-left. The aspheric lens is used to focus as much light as possible on the power meter. To measure the optical power channel by channel, we use a spatial filter with four apertures. All other than the selected beam aperture are blocked during the measurement so that only the selected beam reaches the power meter. The measured optical power can be seen in Figure 3:bottom-right. It is found that the maximum output optical power (at 100 mA laser drive current) is around 140 μW. These values are higher than our previous demonstrators, but not significantly higher. Output powers at different channels can be different. Many reasons may cause these power deviations. For example, non-ideal optical splitters and antennas, or an asymmetric optical system can cause such problems. In later discussions, the input optical power is always set at 80 mA.

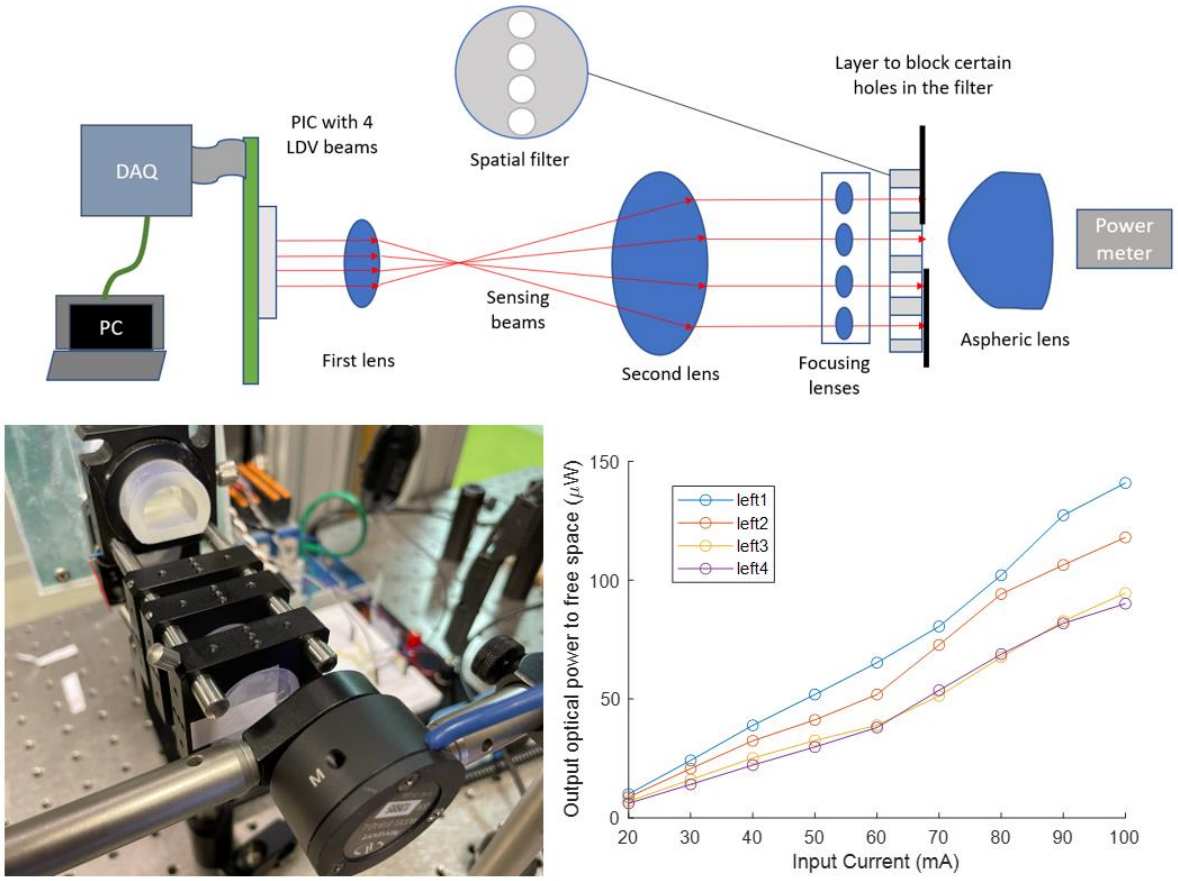

Figure 3. (*Top)*: Schematic drawing of the system measuring optical power from each channel. (*Bottom-left)*: a photo of the measurement setup with a photo-detector from a power meter. (*Bottom-right)*: Measured optical power of each beam as a function of injecting current to the laser diode in the MOB.

We then place the optical spatial filter with different working distances in front of the focusing lenses. A human thumb is then placed on the spatial filter to introduce the reflection from human skin. During each measurement, the filter is fixed to the cage system to ensure that the relative distance between the thumb and the LDV is stable (see Figure 4). During the measurement, the thumb is slightly moving along the optical axis of the lens system. The small movement of the thumb is good enough to form a complete IQ curve. One generated IQ curve is shown in Figure 4:*right*. It is clearly open, which means that the SNR of this signal is good enough for further processing.

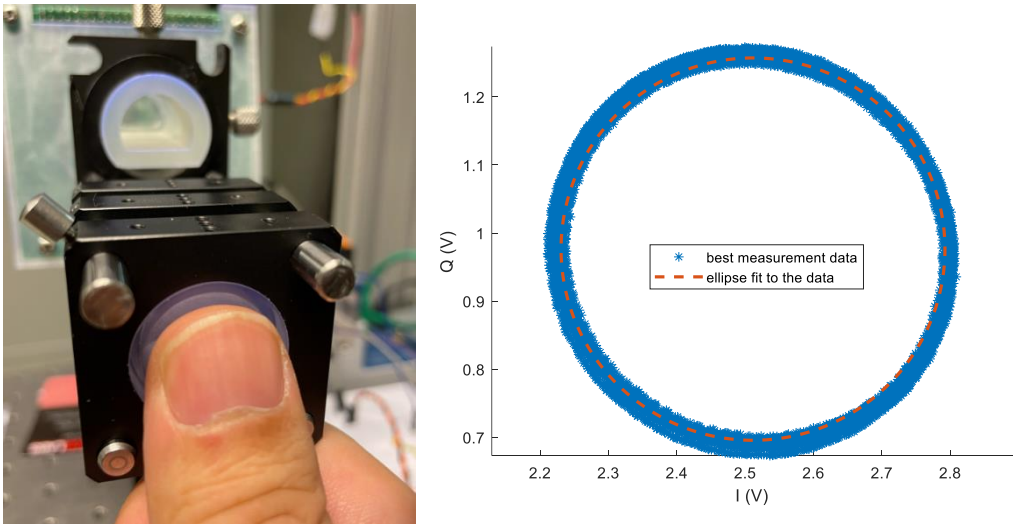

Figure 4. (*Left)*: Test system of the thumb reflection. (*Right)*: one IQ curve generated by the reflection from a bare human thumb.

A typical problem in an LDV interferometer is the nonlinearity caused by an IQ curve that is not an ideal circle. Most of the time, the curve becomes an elliptical shape. This can be caused by an imperfect optical hybrid and imbalanced PD responsivities in the system. The nonlinear effect of the system is estimated with an ellipse fitting of the IQ curve. This can be compensated with certain methods such as Heydemann's method [8].

The IQ curve and the IQ radius as functions of the working distance are shown in Figure 5. Nine IQ curves are plotted in Figure 5(left), which correspond to the reflection signal from 9 different working distances (from 4 mm to 12 mm). The noise floor of the IQ data is around $3 \times 10^{-3} V$ in these IQ curves, which means the SNR of the IQ data ($=Radius/rms\_noise$) can reach 90 when the radius becomes 0.29 V (the green curve in Figure 5 (left)). The plot of the square of IQ radius as a function of working distance is shown in Figure 5 (right). The reason to use a square is that the IQ radius is proportional to the amplitude of reflected optical power. The impact of the depth of focus of the optical system can be clearly seen in this figure. The full-width half-maximum (FWHM) is around 0.8 mm. A fitting function with a profile of $f(x) = 1/(1 + \frac{x^2}{(0.4\text{ mm})^2})$ is placed in the same figure as a comparison. It is also shown that the IQ radius is not symmetric.

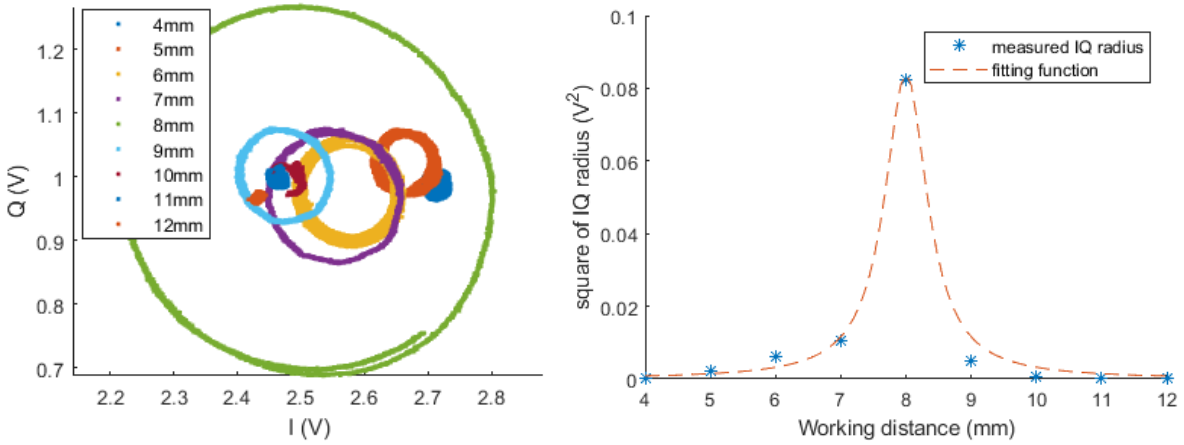

Figure 5. (*left*): IQ curves of the reflections from a bare thumb with different working distances: from 4 mm to 12 mm. (*right*): The IQ radius as a function of the working distance compared to a Gaussian profile with an $\alpha = 0.8$ mm.

It is difficult to measure the noise floor of the demodulated displacement signals from the thumb measurement because the movement of the thumb cannot be standardized (e.g. a sinusoidal signal). To retrieve the relation between the displacement noise and IQ radius, we measured a white paper attached to a small loudspeaker. The loudspeaker generates sound with a single vibration frequency of 800 Hz. The noise floor of these measurement results is estimated by calculating the noise within a small band near 10 kHz, and the bandwidth is 400 Hz. The relation between the displacement noise density and the IQ radius is plotted in Figure 6. One can see that the noise is lower as the IQ radius increases. When the IQ radius is larger than 0.15 V, the noise density of the demodulated signals at 10 kHz will be lower than 10 pm/sqrt(Hz).

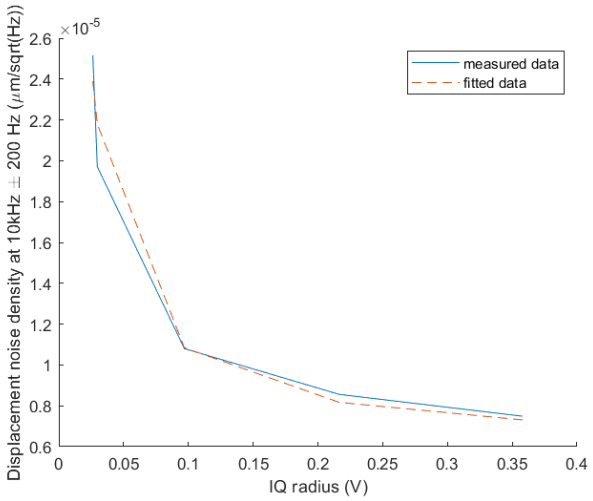

Figure 6. The estimated displacement density as a function of IQ radius. The fitted data are based on the function shown below.

The noise floor can be fitted to the following equation

$$N_{noise-1kHz} = asin\left(\frac{N_r}{Radius}\right) \times \frac{1.31}{4\pi}\mu\text{m} + N_{add},$$

where $N_r = 4.5 \times 10^{-6}$ V/sqrt(Hz), and $N_{add} = 6.0$ pm/sqrt(Hz). The first part of this equation provides the displacement noise transformed from the noise in the IQ data by the demodulation, while the second part is the noise that is irrelevant to radius of the IQ curve, which can be the phase noise. We assume that the noise floor has the same relation when detected on bare skin. Therefore, the expected noise floor for the maximum reflection with the thumb (Radius = 0.29 V) is 7.6 pm/sqrt(Hz). This happens when the thumb is 8 mm away from the focus lens. If the thumb is 1 mm away from the focus center, the expected noise floor increases to 13 pm/sqrt(Hz) (the corresponding Radius =0.07 V). If we use the same noise densities, the total noise of the system over the 50 kHz bandwidth is around 1.7 nm for the focus center. The cross-talks between two adjacent channels are also measured and turn out to be very low.

4. CONCLUSIONS

The resolution of the measurement on bare skin is found to be better than 10 pm/sqrt(Hz) at an 80 mA DFB-laser current when a bare skin surface is placed at the focal plane of the sensing beams. The full-width half-maximum of the working distance is a round 0.8 mm. Based on a data SNR of 90, it can be concluded that the demonstrator can measure vibrations from bare skin. The noise floor at 10 kHz is around 7.6 pm/sqrt(Hz) if the skin is in the focus plane. These improvements are mainly associated with the use of a better numerical aperture in the optical system, the use of better electronics, and the change in the sensing wavelength.

Acknowledgment

This work is supported by the European Horizon 2020 project InSiDe (Grant ID: 871547)

REFERENCES

[1] World Health Organization, Cardiovascular diseases (CVDs) – key facts, website link: https://www.who.int/en/news-room/fact-sheets/detail/cardiovascular-diseases-(cvds), 11 June 2021

[2] Jian Lin, Rumin Fu, Xinxiang Zhong, Peng Yu, Guoxin Tan, Wei Li, Huan Zhang, Yangfan Li, Lei Zhou, Chengyun Ning, Wearable sensors and devices for real-time cardiovascular disease monitoring, Cell Reports Physical Science, 2(8) 100541 (2021)

[3] Santo, K., Redfern, J. Digital Health Innovations to Improve Cardiovascular Disease Care. Curr Atheroscler Rep 22, 71 (2020).

[4] Y. Li, L. Marais, H. Khettab, Z. Quan, S. Aasmul, R. Leinders, R. Schuler, P. Morrissey, S. Greenwald, P. Segers, M. Vanslembrouck, R. Bruno, P. Boutouyrie, P. O'Brien, M. de Melis, R. Baets, Silicon photonics-based laser Doppler vibrometer array for carotid-femoral pulse wave velocity (PWV) measurement, Biomedical Optics Express, 11(7) 3913-3926 (2020)

[5] W. Bogaerts, R. Baets, P. Dumon, V. Wiaux, S. Beckx, D. Taillaert, B. Luyssaert, J. Van Campenhout, P. Bienstman, D. Van Thourhout, Nanophotonic Waveguides in Silicon-on-Insulator Fabricated with CMOS Technology, Journal of Lightwave Technology (invited), 23(1) 401-412 (2005)

[6] Y. Li, S. Aasmul, P. Morrissey, D. Carey, T. Wotherspoon, P. Zaruba, R. Baets, Optimization of multi-beam silicon photonics based laser Doppler vibrometry for measuring cardiovascular signals on bare skin, Photonics West BiOS, 11621, 116210A (2021)

[7] Y. Li, E. Dieussaert, R. Baets, Miniaturization of Laser Doppler vibrometers - a review, Sensors, 22, 4735 (2022)

[8] P. Heydemann, "Determination and correction of quadrature fringe measurement errors in interferometers," Appl. Opt. 20(19), 3382–3384 (1981)